Advanced Ceramics Progress: Vol. 9, No. 3, (Summer 2023) 38-42

Materials and Energy Research Center

MERC

Contents lists available at ACERP

Advanced Ceramics Progress

Journal Homepage: www.acerp.ir

Original Research Article

Construction of 0D/3D $ZnWO_4$-MoS_2 Heterojunction with Enhanced Charge Carrier Separation for Decomposition of Organic Pollutants under Visible Light Irradiation

Mousa Farhadian [a]*, Mohammad Reza Akbarpour [b]

[a] Assistant Professor, Department of Materials Engineering, Faculty of Engineering, University of Maragheh, Maragheh, East Azerbayjan, Iran.
[b] Professor, Department of Materials Engineering, Faculty of Engineering, University of Maragheh, Maragheh, East Azerbayjan, Iran.

* Corresponding Author Email: m.farhadian@maragheh.ac.ir (M. Farhadian)

URL: https://www.acerp.ir/article_183888.html

ARTICLE INFO

Article History:

Received: 14 October 2023
Revised: 07 November 2023
Accepted: 26 November 2023

Keywords:
MoS_2,
$ZnWO_4$,
Photocatalyst,
Heterojunction

ABSTRACT

In the present research, 0D/3D $ZnWO_4$-MoS_2 heterojunction was prepared through a two-step hydrothermal procedure and applied for degradation of MB dye from aqueous solution under visible light irradiation. XRD and FESEM analyses were conducted to conform the successful incorporation of $ZnWO_4$ nanoparticles into the flowerlike MoS_2 structure. Based on the obtained results, heterojunction with 30% wt. of $ZnWO_4$ revealed the best photocatalytic performance compared to the other heterojunction samples. This improvement is mainly attributed to the p-n heterojunction effect where the photoinduced electrons and holes could can be effectively separated on the different semiconductors, thus facilitating the formation of radical active species and resulting in efficient enhancement of photocatalytic performance. Moreover, the results obtained from DRS analysis confirmed that visible light absorption of the heterojunction samples decreased as the $ZnWO_4$ content exceeded 30% wt., which corresponds to the shielding effect of the UV-responsive $ZnWO_4$ component. Hydroxyle radicals was determined as the main active species responsible for photodecomposition of MB.

https://doi.org/10.30501/acp.2023.419323.1136

1. INTRODUCTION

MoS_2 is a two-dimensional (2D) semiconductor material that has received significant attention owing to its unique properties [1,2]. As a photocatalyst, MoS_2 can absorb visible light energy to promote chemical reactions, making it a potential solution for energy conversion and environmental remediation. MoS_2 exhibits excellent catalytic activity due to its high surface area, strong adsorption ability, and tunable bandgap [3–5]. Additionally, its layered structure and strong interlayer interactions result in efficient charge separation and transfer [6]. MoS_2-based photocatalysts have been studied due to their wide applications in hydrogen evolution, water splitting, and degradation of organic pollutants [7]. Further research on MoS_2 as a photocatalyst may lead to the development of more efficient and sustainable technologies for various industrial and environmental applications [8]. Although MoS_2 has shown great potential as a photocatalyst, there are still some limitations that need to be addressed. Some of the notable limitations of MoS_2 as a photocatalyst include poor charge carrier mobility, limited light absorption, and chemical instability [9].

As an n-type semiconductor, $ZnWO_4$ has the ability to absorb Ultraviolent (UV) light energy to promote the chemical reactions and degrade the pollutants [10–12]. It enjoys some unique properties including high surface area, stability under harsh conditions, and efficient

Please cite this article as: Farhadian, M, Akbarpour, M. R.“Construction of 0D/3DZnWO4-MoS2 heterojunction with enhanced charge carrier separation for decomposition of organic pollutants under solar light irradiation”, Advanced Ceramics Progress, Vol. 9, No. 3, (2023), 38-42. https://doi.org/10.30501/acp.2023.419323.1136

charge separation, which contributes to its high photocatalytic activity [13]. The combination of $ZnWO_4$ with MoS_2 semiconductors can broaden the absorption spectrum, hence more solar energy consumption. In addition, the $ZnWO_4/MoS_2$ heterojunction can promote charge separation, leading to more efficient electron-hole pair generation. This happens mainly because $ZnWO_4$ has a higher conduction band position than MoS_2, which facilitates the transfer of electrons from MoS_2 to $ZnWO_4$. The combination of $ZnWO_4$ and MoS_2 can improve the stability and durability of the photocatalyst. $ZnWO_4$ has good chemical stability that protects MoS_2 from oxidation or corrosion under harsh reaction conditions [14]. Overall, application of $ZnWO_4$ as a co-catalyst with MoS_2 can lead to improved photocatalytic performance, enhanced charge separation and transfer, and elevated stability and durability.

In this study, 0D $ZnWO_4$ nanoparticles was loaded on 3D flowerlike MoS_2 microspheres and applied for decomposition of Methylen Blue (MB) dye from aqueous solution through simple hydrothermal method. The pure and hybrid photocatalysts were characterized, and their chemical, structural, and optical characteristics were examined.

2. MATERIALS AND METHODS

In this study, $(NH_4)_6Mo_7O_{27}$, CH_4N_2S, $Na_2WO_4.2H_2O$, $Zn(NO_3)_2{\cdot}6(H_2O)$, ammonia solution (25%), and ethanol were purchased from Merck (Germany) and used without further purification.

The flower-like MoS_2 microspheres were synthesized by a one-step hydrothermal reaction using hexaammonium heptamolybdate tetrahydrate and thiourea as the starting materials. In a typical synthesis, 1.24 g of hexaammonium heptamolybdate tetrahydrate and 2.28 g of thiourea were dissolved in 36 ml deionized water under vigorous stirring for 30 min to form a homogeneous solution. The solution was then transferred into a 50 ml Teflon-lined stainless-steel autoclave and sealed tightly, heated at 220 ^oC for 6 h and then, naturally cooled down to room temperature. Black precipitates were collected by centrifugation and washed with distilled water and absolute ethanol for several times, and finally dried in vacuum at 60 °C for 24 h.

To prepare $ZnWO_4/MoS_2$ heterojunction with various weight ratio of $ZnWO_4$ content, $Zn(NO_3)_2.6H_2O$, $Na_2WO_4.2H_2O$, and CTAB were dissolved in the mixed solution of DMF (40 ml)/H_2O (10 ml). Then, 0.4 g MoS_2 was added to the clear solution and ultrasonically treated for 1 h until a homogeneous mixture was obtained. It was then transformed to the teflon-lined stainless steel autoclave and heat-treated at 180 ^oC for 12 h. The final product was filtered, collected, washed three times with ethanol and deionized water, and then dried in vacuum oven at 80 ^oC for 12 h. The $ZnWO_4/MoS_2$ nanocomposites were denoted as 10ZM, 20ZM, 30ZM, and 40ZM, where the number represents the weight percent of loaded $ZnWO_4$ nanoparticles on the surface of MoS_2.

3. RESULTS AND DISCUSSION

3.1. FE-SEM images

Figure 1 represents the SEM images of MoS_2 flower-like microspheres and $ZnWO_4/MoS_2$ heterojuntion sample with 30 wt.% $ZnWO_4$ content (M30Z). As shown in Figures 1a and 1b, the hierarchical MoS_2 flowerlikes with approximately 1 μm in diameter are formed. In addition, $ZnWO_4$ nanoparticles of approximately 20 nm in diameter are homogeneously integrated among the MoS_2 layers, as demonstrated in Figures 1c and 1d. In these figures, the MoS_2 microflowers retained their original shapes after their combination with $ZnWO_4$ nanoparticles, representing excellent stability of the prepared MoS_2 hierarchical microstructures.

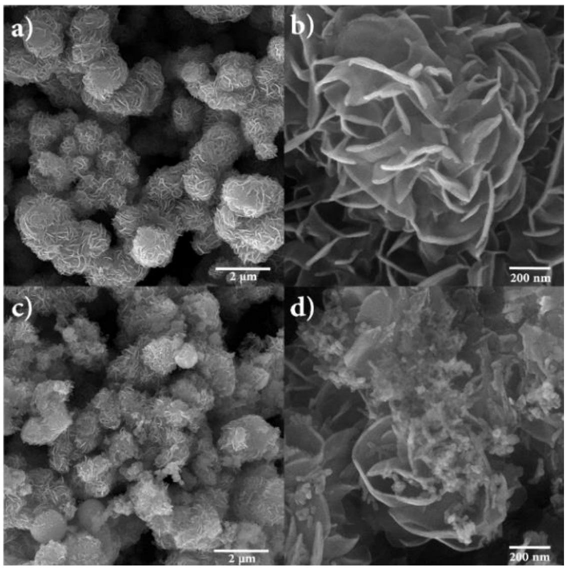

Figure 1. FESEM images of (a, b) MoS_2 microsphere and (c, d) $ZnWO_4/MoS_2$ heterojunction

3.2. XRD

XRD analysis was conducted to study the phase structure of the prepared samples. As seen in Figure 2, the peaks at 2θ=14.5° (002), 34.2° (100), 39.0° (103), 49.5° (105), and 59.0° (110) are attributed to the hexagonal structure of MoS_2 (JPCDS No.00.037-1492). The peaks observed in the XRD pattern of pure $ZnWO_4$ can be attributed to its monoclinic phase (JPCDS No.00.015-0774). Further, the detected peaks of $ZnWO_4$ appear in the XRD pattern of the heterojunction samples, indicating the successful combination of $ZnWO_4$ nanoparticles with the MoS_2 structure. No other peaks are detected in the XRD patterns of heterojunction samples, confirming the formation of the composite samples with no other impurities.

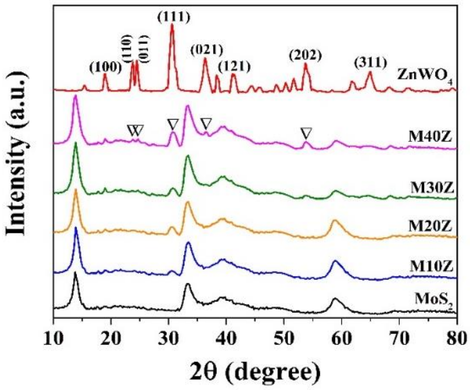

Figure 2. XRD patterns of the pure and heterojunction samples.

3.3 Optical properties

The optical properties of the prepared samples were measured by Diffuse Reflectance Spectroscopy (DRS). As observed in Figure 3, compared with pure MoS_2, the optical absorption edge of the heterojunction samples was shifted to the shorter wavelengths as the $ZnWO_4$ content increased which is attributed to the larger band gap of $ZnWO_4$, indicating the construction of heterojunction at the interface of MoS_2 and $ZnWO_4$. The energy band gap (E_g) of the samples was calculated using Kubelka-Munk equation $(\alpha h\upsilon)^n = A(h\upsilon - Eg)$, the obtained results of which are represented in Figure 4. Accordingly, Eg of heterojunction samples increased upon increasing the $ZnWO_4$ content, compared to pristine MoS_2. The presence of both MoS_2 with narrow band gap and $ZnWO_4$ as a UV-responsive semiconductor benefits broader light absorption and heterojunction effect, which ultimately improve the photocatalytic performance.

3.4 Photocatalytic activity

The photocatalytic performance of the samples was evaluated through photodecomposition of MB from aqueous solution under visible light irradiation. The obtained results are shown in Figure 5. Apparently, MoS_2 exhibits poor photocatalytic activity mainly due to the fast recombination rate of the electron-hole pairs, resulting from its narrow band gap. However, as $ZnWO_4$ is loaded on the surface of MoS_2 structure, the photodegradation activity is enhanced. This improvement results from the heterojunction effect where the produced electrons and holes in MoS_2 can be effectively separated and then, the lifespan of the charge carriers is prolonged, thus facilitating the formation of active species. As seen, photocatalytic decomposition of MB increased up to 30% wt. $ZnWO_4$ content and then decreased. Indeed, $ZnWO_4$ component is not able to absorb visible light spectrum due to its larger band gap. It seems that the higher ZWO_4 nanoparticles loading can cover the optical active sites of the MoS_2 hierarchical and decrease the visible light absorption (Figure 3), resulting in the degraded photocatalytic performance of the M40Z heterojunction sample. To evaluate the stability of the optimum sample (M30Z), recycling experiments were conducted and shown in Figure 6. The results revealed that the photocatalytic degradation percentage of the M30Z sample only decreased approximately 5%, showing good chemical stability.

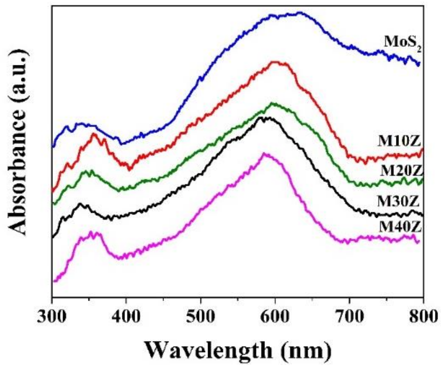

Figure 3. DRS plots of pure MoS_2 and prepared heterojunctions.

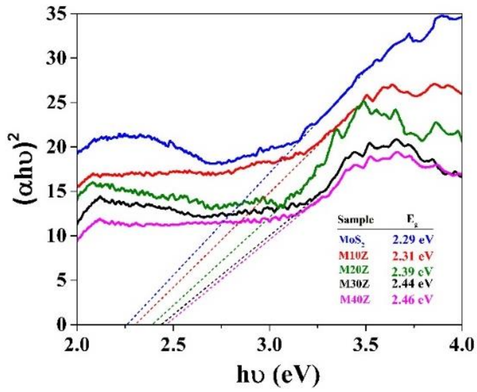

Figure 4. Tauc Plots of pure MoS_2 and prepared heterojunctions.

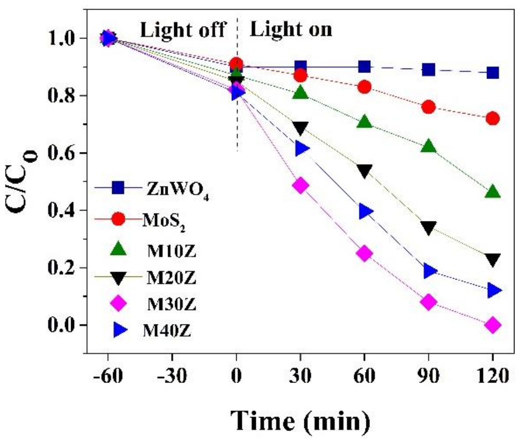

Figure 5. Photocatalytic decomposition of MB from aqueous solution over prepared pure and heterojunction samples under visible light irradiation.

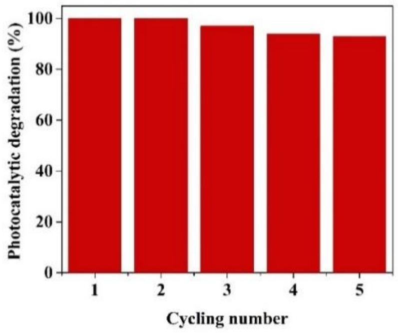

Figure 6. Recycling evaluation of M30Z sample toward MB decomposition under visible light irradiation.

3.5 Photocatalytic mechanism

To study the photocatalytic mechanism of the prepared heterojunction, radical trapping experiments were conducted to determine the active species responsible for the photocatalytic degradation of MB. To this end, triethanolamine (TEA), benzoquinone (BQ), and isopropyl alcohol (IPA) were separately added as the scavengers of holes, superoxide radicals and hydroxide radicals, respectively. As shown in Figure 7, the photodegradation of MB was slightly reduced in the presence of BQ, indicating that the superoxide radicals had no significant role in the photocatalytic decomposition of MB. In addition, the significant reduction in the photocatlytic performance in the presence of IPA denote that hydroxyle radicals are the main species for photodecomposition of MB. In addition, the photoinduced holes are also involved in the photodegradation of MB.

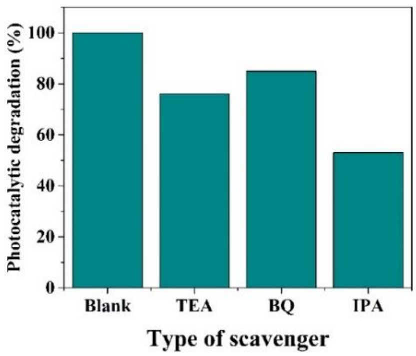

Figure 7. Photocatalytic degradation of MB in the presence of various scavengers.

4. CONCLUSION

In summary, hierarchical $ZnWO_4$-MoS_2 heterojunction samples with different $ZnWO_4$ contents were successfully prepared by a simple two-step hydrothermal method, and served toward photocatalytic degradation of MB dye from aqueous solutions under visible light irradiation. Based on the obtained results, $ZnWO_4$-MoS_2 heterojunction with 30 mol. % content of $ZnWO_4$ revealed 8.33 times enhancement after 120 min irradiation compared to pure MoS_2. This improvement is mainly attributed to the heterojunction effect during which, photoinduced electrons and holes over MoS_2 were effectively separated and easily participated for the radical species production. Further, recycling experiments showed that the fabricated $ZnWO_4$-MoS_2 revealed only around 5% reduction in the MB photodegradation which represents that sufficient numbers of bonding are formed at their interface. Further, the results indicated that hydroxyle radical along with the photoinduced holes are the main species toward photocatalytic degradation of MB. The obtained results verify that the prepared $ZnWO_4$-MoS_2 heterojunction can be a promising visible-light-activated photocatalyst for efficient degradation of dye contaminants from wastewater.

ACKNOWLEDGEMENTS

The author wish to acknowledge University of Maragheh for the all support throughout this work.

REFERENCES

1. Waghchaure, R. H., Adole, V. A., Jagdale, B. S., & Koli, P. B. (2022). Fe^{3+} modified zinc oxide nanomaterial as an efficient, multifaceted material for photocatalytic degradation of MB dye and ethanol gas sensor as part of environmental rectification. ***Inorganic Chemistry Communications***, 140, 109450. https://doi.org/10.1016/j.inoche.2022.109450
2. Khan, I., Saeed, K., Zekker, I., Zhang, B., Hendi, A. H., Ahmad, A., ... & Khan, I. (2022). Review on methylene blue: Its properties, uses, toxicity and photodegradation. ***Water***, 14(2), 242. https://www.mdpi.com/2073-4441/14/2/242#
3. Bahadoran, A., Farhadian, M., Hoseinzadeh, G., & Liu, Q. (2021). Novel flake-like Z-Scheme Bi_2WO_6-$ZnBi_2O_4$ heterostructure prepared by sonochemical assisted hydrothermal procedures with enhanced visible-light photocatalytic activity. ***Journal of Alloys and Compounds***, 883, 160895. https://doi.org/10.1016/j.jallcom.2021.160895
4. Koli, P. B., Kapadnis, K. H., Deshpande, U. G., & Patil, M. R. (2018). Fabrication and characterization of pure and modified Co $_3O_4$ nanocatalyst and their application for photocatalytic degradation of eosine blue dye: a comparative study. ***Journal of Nanostructure in Chemistry***, 8, 453-463. https://doi.org/10.1007/s40097-018-0287-0
5. Ahire, S. A., Bachhav, A. A., Jagdale, B. S., Patil, A. V., Koli, P. B., & Pawar, T. B. (2023). Amalgamation of ZrO_2-PANI Nanocomposite Polymeric Material: Characterization and Expeditious Photocatalytic Performance Towards Carbol Fuchsin (CF) Dye and Kinetic Study. ***Journal of Inorganic and Organometallic Polymers and Materials***, 33(5), 1357-1368. https://doi.org/10.1007/s10904-023-02590-3
6. Koli, P. B., Kapadnis, K. H., & Deshpande, U. G. (2019). Transition metal decorated Ferrosoferric oxide (Fe_3O_4): An expeditious catalyst for photodegradation of Carbol Fuchsin in environmental remediation. ***Journal of Environmental Chemical Engineering***, 7(5), 103373. https://doi.org/10.1016/j.jece.2019.103373
7. Koli, P. B., Shinde, S. G., Kapadnis, K. H., Patil, A. P., Shinde, M. P., Khairnar, S. D., ... & Ingale, R. S. (2021). Transition metal incorporated, modified bismuth oxide (Bi_2O_3) nano photo catalyst for deterioration of rosaniline hydrochloride dye as resource for environmental rehabilitation. ***Journal of the Indian Chemical Society***, 98(11), 100225. https://doi.org/10.1016/j.jics.2021.100225

8. Li, W., Wang, L., Zhang, Q., Chen, Z., Deng, X., Feng, C., ... & Sun, M. (2019). Fabrication of an ultrathin 2D/2D C_3N_4/MoS_2 heterojunction photocatalyst with enhanced photocatalytic performance. ***Journal of Alloys and Compounds***, 808, 151681. https://doi.org/10.1016/j.jallcom.2019.151681
9. Khalid, N. R., Kamal, M. R., Tahir, M. B., Rafique, M., Niaz, N. A., Ali, Y., ... & Muhammad, S. (2021). Fabrication of direct Z-scheme MoO_3/N–MoS_2 photocatalyst for synergistically enhanced H_2 production. ***International Journal of Hydrogen Energy***, 46(80), 39822-39829. https://doi.org/10.1016/j.ijhydene.2021.09.230
10. Li, Z., Meng, X., & Zhang, Z. (2018). Recent development on MoS_2-based photocatalysis: A review. Journal of Photochemistry and Photobiology C: ***Photochemistry Reviews***, 35, 39-55. https://doi.org/10.1016/j.jphotochemrev.2017.12.002
11. Sun, J., Li, X., Guo, W., Zhao, M., Fan, X., Dong, Y., ... & Fu, Y. (2017). Synthesis methods of two-dimensional MoS_2: A brief review. ***Crystals***, 7(7), 198. https://www.mdpi.com/2073-4352/7/7/198#
12. Liang, Z., Shen, R., Ng, Y. H., Zhang, P., Xiang, Q., & Li, X. (2020). A review on 2D MoS_2 cocatalysts in photocatalytic H_2 production. Journal of Materials Science & Technology, 56, 89-121. https://doi.org/10.1016/j.jmst.2020.04.032
13. Huang, S., Chen, C., Tsai, H., Shaya, J., & Lu, C. (2018). Photocatalytic degradation of thiobencarb by a visible light-driven MoS_2 photocatalyst. ***Separation and Purification Technology***, 197, 147-155. https://doi.org/10.1016/j.seppur.2018.01.009
14. Yuan, Y. J. *et al*. "The role of bandgap and interface in enhancing photocatalytic H_2 generation activity of 2D-2D black phosphorus/MoS_2 photocatalyst", ***Applied Catalysis B: Environmental***, Vol. 242, (2019), 1–8. https://doi.org/10.1016/j.apcatb.2018.09.100
15. Yuan, Y., Guo, R. T., Hong, L. F., Ji, X. Y., Li, Z. S., Lin, Z. D., & Pan, W. G. (2021). Recent advances and perspectives of MoS_2-based materials for photocatalytic dyes degradation: a review. Colloids and Surfaces A: Physicochemical and Engineering Aspects, 611, 125836. https://doi.org/10.1016/j.colsurfa.2020.125836
16. Cui, E., Yu, G., Huang, H., & Li, Z. (2017). Current advances in MoS_2/semiconductor heterojunction with enhanced photocatalytic activity. ***Current Opinion in Green and Sustainable Chemistry***, 6, 42-47. https://doi.org/10.1016/j.cogsc.2017.05.009
17. Abubakar, H. L., Tijani, J. O., Abdulkareem, S. A., Mann, A., & Mustapha, S. (2022). A review on the applications of zinc tungstate ($ZnWO_4$) photocatalyst for wastewater treatment. Heliyon. https://doi.org/10.1016/j.heliyon.2022.e09964
18. Fu, H., Lin, J., Zhang, L., & Zhu, Y. (2006). Photocatalytic activities of a novel $ZnWO_4$ catalyst prepared by a hydrothermal process. ***Applied Catalysis A: General***, 306, 58-67. https://doi.org/10.1016/j.apcata.2006.03.040
19. Andrade, A. O., da Silveira Lacerda, L. H., Júnior, M. L., Sharma, S. K., da Costa, M. M., Alves, O. C., ... & Almeida, M. A. (2023). Enhanced photocatalytic activity of BiOBr/$ZnWO_4$ heterojunction: A combined experimental and DFT-based theoretical approach. ***Optical Materials***, 138, 113701. https://doi.org/10.1016/j.optmat.2023.113701
20. Rathi, V., Panneerselvam, A., & Sathiyapriya, R. (2020). Graphitic carbon nitride (g-C_3N_4) decorated $ZnWO_4$ heterojunctions architecture synthesis, characterization and photocatalytic activity evaluation. ***Diamond and Related Materials***, 108, 107981. https://doi.org/10.1016/j.diamond.2020.107981
21. Atla, R., & Oh, T. H. (2021). Solar light-driven 2D MoS_2 nanoflake-supported 1D $ZnWO_4$ nanorod heterostructure: Efficient separation of charge carriers for removing toxic organic pollutants. ***Journal of Environmental Chemical Engineering***, 9(6), 106427. https://doi.org/10.1016/j.jece.2021.106427
22. Liang, L., Liu, H., Tian, Y., Hao, Q., Liu, C., Wang, W., & Xie, X. (2016). Fabrication of novel $CuWO_4$ hollow microsphere photocatalyst for dye degradation under visible-light irradiation. ***Materials Letters***, 182, 302-304. https://doi.org/10.1016/j.matlet.2016.05.166
23. Geetha, G. V., Sivakumar, R., Sanjeeviraja, C., & Ganesh, V. (2021). Photocatalytic degradation of methylene blue dye using $ZnWO_4$ catalyst prepared by a simple co-precipitation technique. ***Journal of sol-gel science and technology***, 97, 572-580. https://doi.org/10.1007/s10971-021-05480-7
24. Geetha, G. V., Keerthana, S. P., Madhuri, K., & Sivakumar, R. (2021). Effect of solvent volume on the properties of $ZnWO_4$ nanoparticles and their photocatalytic activity for the degradation of cationic dye. ***Inorganic Chemistry Communications***, 132, 108810. https://doi.org/10.1016/j.inoche.2021.108810
25. Rani, A., Singh, K., Patel, A. S., Chakraborti, A., Kumar, S., Ghosh, K., & Sharma, P. (2020). Visible light driven photocatalysis of organic dyes using SnO_2 decorated MoS_2 nanocomposites. ***Chemical Physics Letters***, 738, 136874. https://doi.org/10.1016/j.cplett.2019.136874
26. Kao, L. H., Chuang, K. S., Catherine, H. N., Huang, J. H., Hsu, H. J., Shen, Y. C., & Hu, C. (2023). MoS_2-coupled coniferous ZnO for photocatalytic degradation of dyes. ***Journal of the Taiwan Institute of Chemical Engineers***, 142, 104638. https://doi.org/10.1016/j.jtice.2022.104638